AD-A160 699 A SIMS STUDY OF THE INFLUENCE OF LOW LEVELS OF SILICON AND CALCIUM ON THE..(U) TEXAS UNIV AT AUSTIN DEPT OF CHEMISTRY S AKHTER ET AL. 15 OCT 85 TR-43 1/1

UNCLASSIFIED N00014-83-K-0582 F/G 7/4 NL

END

FILMED

DTIC

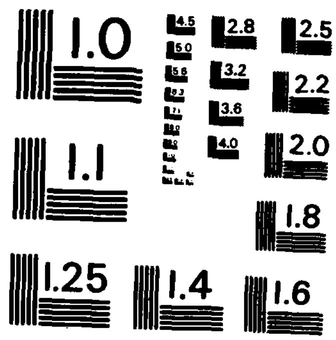

MICROCOPY RESOLUTION TEST CHART
NATIONAL BUREAU OF STANDARDS-1963-A

(12)

OFFICE OF NAVAL RESEARCH

Contract No. N00014-83-K-0582

Task No. NR 056-578

TECHNICAL REPORT NO. 43

A SIMS Study of the Influence of Low Levels of Silicon and Calcium on the Adsorption Properties of O_2 on Pt(111)

by

S. Akhter, C. M. Greenlief, H.-W. Chen and J. M. White

Prepared for publication

in

Applied Surface Science

Department of Chemistry

The University of Texas at Austin

Austin, Texas 78712

SECURITY CLASSIFICATION OF THIS PAGE (When Data Entered)

REPORT DOCUMENTATION PAGE

READ INSTRUCTIONS BEFORE COMPLETING FORM

1. REPORT NUMBER

2. GOVT ACCESSION NO. AD-A160 699

3. RECIPIENT'S CATALOG NUMBER

4. TITLE (and Subtitle)

A SIMS Study of the Influence of Low Levels of Silicon and Calcium on the Adsorption Properties of O_2 on Pt(111)

5. TYPE OF REPORT & PERIOD COVERED

Technical Report 43
January 1 - December 31, 1985

6. PERFORMING ORG. REPORT NUMBER

7. AUTHOR(s)

S. Akhter, C. M. Greenlief, H.-W. Chen and J. M. White

8. CONTRACT OR GRANT NUMBER(s)

N00014-83-K-0582

9. PERFORMING ORGANIZATION NAME AND ADDRESS

J. M. White, Department of Chemistry
University of Texas
Austin, TX 78712

10. PROGRAM ELEMENT, PROJECT, TASK AREA & WORK UNIT NUMBERS

Project No. NR-056-578

11. CONTROLLING OFFICE NAME AND ADDRESS

Department of the Navy
Office of Naval Research
Arlington, VA 22217

12. REPORT DATE

October 15, 1985

13. NUMBER OF PAGES

12

14. MONITORING AGENCY NAME & ADDRESS (if different from Controlling Office)

15. SECURITY CLASS. (of this report)

15a. DECLASSIFICATION/DOWNGRADING SCHEDULE

16. DISTRIBUTION STATEMENT (of this Report)

Approved for public release; distribution unlimited.

17. DISTRIBUTION STATEMENT (of the abstract entered in Block 20, if different from Report)

18. SUPPLEMENTARY NOTES

Preprint: Appl. Surface. Sci. (in press)

19. KEY WORDS (Continue on reverse side if necessary and identify by block number)

20. ABSTRACT (Continue on reverse side if necessary and identify by block number)

Surface impurity levels of Ca, Si and Al at or below the detectability limits of AES were followed in SIMS and correlated with oxygen adsorption on Pt(111). It is shown that oxidation of Si to SiO_x, monitored by the rise in SIMS Si^+ ion intensity, takes place above 500K during oxygen TPD. SiO_x starts decomposing above 1100K and can be reduced within 200 sec by 2×10^{-8} torr of H_2 at 1200K. The O_2 adsorbed/desorbed in a TPD cycle depends on the immediate history of the impurity levels on the surface. SiO_x presence correlates with an increase in the overall oxygen sticking coefficient. These results highlight the importance of impurity levels below AES detectability and suggest pretreatment methods for obtaining better reproducibility.

DD FORM 1 JAN 73 1473 EDITION OF 1 NOV 65 IS OBSOLETE
S/N 0102-014-6601

SECURITY CLASSIFICATION OF THIS PAGE (When Data Entered)

2

A SIMS STUDY OF THE INFLUENCE OF LOW LEVELS OF SILICON AND CALCIUM ON THE ADSORPTION PROPERTIES OF O_2 ON Pt(111)[a]

S. Akhter, C. M. Greenlief, H.-W. Chen and J. M. White

Department of Chemistry

University of Texas

Austin, Texas 78712

(a) Supported in part by the Office of Naval Research.

ABSTRACT

Surface impurity levels of Ca, Si and Al, which are at or below the detectability limits of Auger electron spectroscopy, have been followed in secondary ion mass spectrometry (SIMS) and correlated with oxygen adsorption on Pt(111). It is shown that oxidation of Si to SiO_x, monitored by the rise in the SIMS Si^+ ion intensity, takes pla e above 500 K during oxygen TPD. The SiO_x starts decomposing above 1100 K and can be reduced within 200 secs. by $2x10^{-8}$ torr of H_2 at 1200 K. The molecular, atomic and total amount of oxygen adsorbed/desorbed in a temperature programmed desorption (TPD) cycle depends on the immediate past history of the impurity levels on the surface. In particular, the presence of SiO_x is correlated with an increase in the overall sticking coefficient of oxygen. These results highlight the importance of impurity levels below the detectability limits of AES and suggest pretreatment methods for obtaining better reproducibility.

1. INTRODUCTION

There have been a number of reports regarding the role of Si in the formation of the high temperature "oxide" state on Pt(111) and the catalytic properties of that state. The various findings have been summarized [1-3]. Following the work of Neihus and Comsa[1, 2] and Bonzel et al.[3], it became clear that a Pt(111) surface could be considered clean if, after oxidation at ≈1000 K, no oxide state(due to Si) could be detected in AES. Typically a surface is deemed "clean" by AES if impurity levels are below its detectability limits(~ 0.01 ML). While this may be acceptable in most cases, it is, nevertheless, important to characterize impurities at even lower levels and to examine their significance in surface processes.

Several other interesting observations have been attributed to Si or SiO_x. Segner et al. [4] reported better thermal accomodation of CO_2 with a Pt(111) surface in the presence of the "oxide" state. Another interesting observation made by Mundschau and Vanselow [7] is that the silicon impurity in platinum can stabilize (210) planes on a field emitter tip. Yeates et al. [6] report that the presence of silicon was necessary to observe oscillatory behavior during CO oxidation on Pt(111) at atmospheric pressure.

Recently, we have been engaged in using secondary ion mass spectrometry (SIMS) as a tool for kinetic studies. In the course of these studies on Pt(111), we noted variations in the impurity ion levels in static SIMS, depending on the immediate past history of the sample, although, by AES, the surface was considered clean and no changes could be observed. Oxygen

desorption areas from this surface, after different pretreatments, showed variations as high as 30%, even if all experiments were done within an hour. This pointed to a significant effect of impurities, which were at or below Auger detectability limits.

We report here a systematic study of the silicon, calcium and aluminum positive SIMS signals and their variation with oxygen and hydrogen dosing and with argon sputtering treatments of the platinum surface. The desorption of oxygen is correlated with the levels of these signals.

In the previous investigations of Niehus and Comsa[1, 2] and Bonzel et al.[3], the following important observations were made:

(a) The location of Si and SiO_x is subsurface at low concentrations.

(b) The equilibrium amount of segregated Si declines rapidly above 900 K.

(c) The rate of segregation is very slow below 900 K.

(d) The equilibrium amount, but not the rate, of segregated Si is enhanced in the presence of oxygen.

(e) The presence of Si could be more reliably inferred from the presence of the AES oxygen peak after oxidizing Si to SiO_x than from AES of Si.

These observations provided a framework on which our experimental design is based. It should be pointed out that in the above investigations, large amounts of Si were deposited and diffused in the bulk. In the present report, small variations in Si and other impurity levels were achieved by heating the sample at 1200 K for variable times. In the following sections, the Si that is accessible to oxygen and affects its adsorption properties, is simply referred to as "surface silicon".

2. EXPERIMENTAL

The experiments were performed in a turbo-pumped UHV system equipped with a double pass CMA for AES and a quadrupole mass spectrometer having SIMS capabilities. Pressures of 3×10^{-10} Torr were regularly obtained. The Pt(111) sample could be heated to 1300 K and cooled to 100 K with liquid nitrogen. The temperature was measured with a chromel-alumel thermocouple. The SIMS spectra were taken in line-of-sight of the quadrupole with a 600 eV beam of less than 2 nA of Ar^+ current rastered over the surface.

3. RESULTS AND DISCUSSION

3.1 The SIMS Si^+ ion

Fig. 1 shows typical SIMS and AES spectra of a "clean" surface, selected arbitrarily out of our data. The SIMS spectrum shows a number of impurity ions including Na^+, Mg^+, Al^+, Si^+, K^+ and Ca^+. The Al^+, Si^+ and Ca^+ ions were always present and it was not possible to eliminate them completely. The AES spectrum shows no evidence of these impurities (AES impurity/substrate ratio <0.01). In particular, the absence of Si and O (due to SiO_x) are noted. The inset shows the <u>maximum</u> amount of "oxide"(O/Pt_{237} = 0.08) that was ever seen during the experiments reported here.

At the outset we ask whether the Si^+ ion is from elemental Si or SiO_x. We have focused on the Si impurity because of its known affinity for oxygen on Pt(111). To resolve this issue, the surface was heated in vacuum at

1000 K for 15 minutes and oxidized to segregate as much SiO_x as possible. The segregated SiO_x was then partially reduced to Si by heating in 2×10^{-8} torr of H_2 at 1200 K for 200 secs. The temperature was then decreased to 650 K. The SIMS Si^+ count on this surface is shown by the initial portion (0 to 100 secs.) of the curve in Fig. 2. The Auger scans of the O(KLL) and Pt(237) regions are also shown. The surface was then exposed to 2×10^{-8} torr of oxygen at 650 K. The Si^+ signal increased immediately upon exposure and slowly saturated. Since the diffusion of Si to the surface at 650 K is very slow [3], the observed increase in Si^+ signal is ascribed to the oxidation of pre-existing surface silicon to SiO_x. This was confirmed by flashing off only the adsorbed oxygen. The Si^+ signal did not change. Thus we conclude that the enhancement described above was due to SiO_x, not chemisorbed oxygen. Furthermore, an AES scan taken after flashing off adsorbed oxygen (1000 K) shows a small amount of residual oxygen, attributed to the "oxide" state (Fig. 2). This confirms the presence of SiO_x and also suggests a relation between the Si^+ ion intensity and the presence of the oxide state. We conclude that for very low levels of silicon on Pt(111), the SIMS Si^+ ion is predominantly from SiO_x and can be used as a measure of the SiO_x concentration. The Si concentration can be indirectly measured by completely oxidizing it to SiO_x at low temperatures. Further evidence for our conclusion will become apparent during later discussions.

3.2 Formation and stability of SiO_x

SiO_x can be formed by continuous exposure of the surface to oxygen above 400 K [3], as shown in Fig. 2. It also forms during an oxygen TPD cycle. In Fig. 3, oxygen was adsorbed, at 100 K, on a Pt(111) surface, which had been subjected to one adsorption/desorption cycle after sputtering

and annealing. The temperature was ramped at 5.5 K/s to 1060 K and held there for a few minutes. The Si^+ ion intensity gradually increases up to about 900 K. Again, the increase is attributed to the oxidation of Si to SiO_x because the diffusion of Si to the surface is very slow at lower temperatures. The increase in Si^+ intensity above 500 K is also consistent with the fact that O(a) becomes mobile above that temperature [5] and thus is able to react with Si more readily.

The SiO_x also yields the $^{28}Si^{16}O^+$ ion (m/e = 44) which was confirmed by oxidizing in $^{18}O_2$, after which the $^{28}Si^{18}O^+$ ion (m/e = 46) was observed . The SiO_x is reasonably stable up to 1100 K, but it starts to decompose at higher temperatures, as evidenced by the decline in both $^{28}Si^+$ and $^{28}Si^{16}O^+$ signals when a surface exhibiting a relatively high Si^+ signal, was temperature programmed (Fig. 4). The decline is not due to diffusion into the bulk, because the Si was initially segregated at a higher temperature (1200 K). Also, most of the Si^+ intensity may be recovered by reoxidizing at low temperatures, which suggests that the Si is still in the surface region. The reason for the peak in the Si^+ intensity before its final decline above 1100 K is not clear. It may be connected with SiO_x rearrangement before decomposition.

Heating in $2x10^{-8}$ torr of H_2 at 1200 K for 200 sec. was sufficient to reduce nearly all the SiO_x to Si, as shown by the disappearance of the Si^+ ion in the SIMS spectra of Fig. 5. For higher concentrations of SiO_x (observable in AES), the above treatment was not sufficient. Longer reduction times and/or sputtering was required to completely remove the SIMS Si^+ signal.

It was also noted that the Ca^{+2} ion (m/e = 20) disappeared upon reduction (after H_2 treatment in Fig. 5) while the Ca^+ ion intensity was

enhanced. This contrasting behavior is reconciled if the Ca^{+2} ion is attributed to CaO (which is present before reduction) and the Ca^+ ion being mainly from elemental Ca. Such a correlation between the charge of the ion and its valence state on the surface has been observed frequently.[9] That the m/e = 40 ion was due to $^{40}Ca^+$ and not $^{39}K^1H^+$ was confirmed by reducing in D_2 (instead of H_2) in which case no m/e = 41 ($^{39}K^2D^+$) ion was observed.

3.3 Oxygen adsorption: Impurities at AES detection limit

A set of experiments was performed to study the dependence of oxygen adsorption on the impurity levels of Si, SiO_x, Ca etc. It was considered neccessary to observe SiO_x in AES, so as to establish its existence and determine an upper limit of its concentration.

The surface was sputtered and then annealed at 1200 K to segregate some silicon. 10 L of oxygen ($1x10^{-7}$ torr, 100 secs.) was adsorbed at 100 K and subsequently desorbed by flashing to 1000 K. After that, the surface was alternately oxidized ($1x10^{-7}$ torr O_2, 700 K, 900 secs.) and reduced ($2x10^{-8}$ torr H_2, 1200 K, 200 secs). After each treatment, an AES scan, a SIMS scan and an oxygen adsorption/desorption cycle were performed. The results are shown in Fig. 6, where the desorbed oxygen amounts and the SIMS and AES impurity signals are plotted against the pretreatment run number (O= oxidation, R= reduction, C= sputter cleaned). A good correlation is observed between the changes in the amount of oxygen desorbed and the variation in the impurity levels as observed by SIMS and AES. It is noted that oxidation to form SiO_x (increase in Si^+ intensity) leads to an increase in oxygen desorption. Reduction produces Si (decline in Si^+) and a decrease in O_2 desorbed. The O/Pt(237) ratio corresponding to the "oxide" state is also shown. The maximum value of this ratio in these experiments was 0.08.

A good correlation between the maxima in the O/Pt ratio and the maxima in the Si^+ counts is also noted.

The Al^+ ion behaves like the Si^+ ion. The Ca^+ ion intensity, on the other hand, decreased upon oxidation and increased on reduction. This might suggest that the Ca^+ intensity is primarily due to elemental Ca (Ca^+ ion yield is not enhanced by oxygen). In the AES scans, Ca and Al were not seen, except in the second oxidation experiment of Fig. 6, where a small amount of Ca was detected ($Ca/Pt_{237} = 0.03$).

From the present set of experiments, we conclude that the oxygen adsorption/desorption properties of Pt(111) are dependent on the immediate past history of the impurity levels. We tentatively attribute the above variations in oxygen uptake to alternate oxidation and reduction of Si, although we cannot rule out effects due to Ca and Al. We note, however, that the changes in oxygen adsorption were observed after pretreatments (oxidation and reduction conditions) that are known to effect changes in the chemical state of Si [1-3].

The effect of impurities is further demonstrated by the results of Fig. 7. In this series of experiments, consecutive O_2 adsorption/desorption was performed (7 times), starting from a sputter-cleaned and annealed surface. Before and after each desorption, SIMS spectra were recorded. The O_2 exposure in each experiment was 10 L at 100 K and the TPD was terminated at 1000 K. The desorption areas from the first experiment are arbitrarily set to 100 and, thus, the ordinate represents the per cent increase in desorption area. The results correlate the amount of O_2 desorbed and the intensities of Si^+ (SiO_x), Ca^+ and Al^+ ions. The amount of O_2 desorbed and the Si^+ and Al^+ intensities increase monotonically while the Ca^+ ion intensity decreases continuously. With the considerations outlined above in

mind, we discuss these results in terms of changes in the state of Si. From Fig. 7, the conversion of Si to SiO_x (increase in Si^+ intensity) leads to greater oxygen adsorption in the same adsorption time; that is, the overall sticking coefficient is enhanced in the presence of SiO_x. Alternatively, it may be argued that the presence of Si decreases the overall sticking coefficient. These two effects cannot be separated, based on our results.

After run #6 of Fig. 7, an AES scan revealed a small amount of oxygen due to the "oxide" ($O/Pt_{237} = 0.06$). Before run #7, the sample was heated in H_2 (2×10^{-8} torr, 1200 K, 200 secs.) to reduce SiO_x to Si. Both the Si^+ intensity and the amount of desorbed oxygen decline, as expected from the behavior in preceeding runs.

Our best estimate of the maximum amount of Si present in this series of experiments (evaluated from the O/Pt_{237} ratio after run #6) is 0.025 ML, assuming SiO_2 stoichiometry and an O/Pt_{237} ratio of 0.3 for 0.25 ML O(a) on Pt(111).[8] The latter is reasonable since, for saturation amounts of atomic oxygen, we obtained O/Pt_{237} ratios between 0.3 and 0.4.

The oxygen TPD peak positions were in agreement with previous investigations [8]. The molecular state desorbed in a sharp peak at 140 K and the atomic state desorbed between 640 and 670 K depending on the oxygen coverages attained in the above sequential adsorption experiments. Generally, the peak due to the atomic state became wider and the peak position shifted to lower temperatures as the oxygen uptake increased in each subsequent adsorption. The effect, if any, of Ca, Si and Al on the position and shape of the atomic peak is difficult to discern. All changes are consistent with the second order nature of the atomic peak.

3.4 Oxygen adsorption/desorption: Impurities below AES detectability limits

The dependence of oxygen adsorption on impurity levels below the detectability limits of AES was also investigated. The series of experiments in section 3.3 were repeated on a surface which did not show any detectable "oxide" in AES ($O/Pt_{237} < 0.01$) after 7 oxygen TPD cycles. As before, 10 L of oxygen was adsorbed at 100 K and followed by a TPD to 1000 K. The results are shown in Fig. 8. The data again show that the amount of oxygen desorbed and the Si^+, Ca^+ and Al^+ ion intensities are correlated.

As before, we discuss these results in terms of changes in the state of Si. The overall sticking coefficient of oxygen is enhanced when the Si is oxidized to SiO_x. The major difference between the high impurity level (section 3.3) and low impurity level results is that in the former case the total amount of oxygen desorbed increases by 50% while in the latter the increase is only 15% in going from an unoxidized (elemental Si) to oxidized (SiO_x) surface. Unfortunately, the relative quantities of oxygen desorbed in the two cases (high and low impurity levels) cannot be directly compared because these experiments were done at different times, between which the chamber had been opened, and the detector sensitivity was not the same.

4. CONCLUSIONS

Based on the results discussed above, the following conclusions are made:

(i) A Pt(111) surface deemed "clean" by AES may still contain surface impurities that have a detectable influence on kinetic phenomena. The use of SIMS extends the lower limit of the cleanliness criterion.

(ii) (Near) surface Si is readily oxidized to SiO_x during oxygen TPD. The SIMS Si^+ ion can be used to follow the oxidation process.

(iii) Oxygen adsorption on Pt(111) at 100 K is dependent on the

impurity levels which are determined by the immediate past history of the sample.

(iv) The presence of SiO_x (absence of Si) enhances the overall sticking coefficient of oxygen on Pt(111).

(v) The reproducibility of oxygen uptake improves as the elemental silicon impurity level drops.

These results suggest that cleaning Pt(111) surfaces should involve sputtering with repeated O_2 exposures and SIMS analysis until Si^+ and SiO^+ levels drop to very low values. Residual Si should be oxidized prior to experiments involving oxygen or oxygenated compounds in order to obtain stable adsorption properties.

The presence of SiO_x enhances the uptake of oxygen. The mechanism involved is probably electronic, as the Pt atoms near SiO_x may be considered to be supported on it, as suggested by Neihus and Comsa [1].

REFERENCES

1. H. Niehus and G. Comsa, Surface Sci., 93(1980)L147 and references therein.
2. H. Niehus and G. Comsa, Surface Sci., 102(1981)L14.
3. H. P. Bonzel, A. M. Franken and G. Pirug, Surface Sci., 104(1981)625 and references therein.
4. J. Segner, C. T. Campbell, G. Doyen and G. Ertl, Surface Sci., 138(1984)505.
5. R. Lewis and R. Gomer, Surface Sci., 12(1968)157.
6. R. C. Yeates, J. E. Turner, A. J. Gellman and G. A. Somorjai, Surface Sci., 149(1985)175.
7. M. Mundschau and R. Vanselow, Surface Sci. 155 (1985) 121.
8. J. L. Gland, Surface Sci., 93(1980)487.
9. A. Benninghoven, Surface Sci. 53 (1975) 596.

FIGURE CAPTIONS

Fig. 1: AES and SIMS spectrum of a "clean" Pt(111) surface. A 1.8 nA and 600 eV Ar^+ ion beam was used for the SIMS scan. The inset represents the maximum "oxide" (corresponding to O/Pt_{237} of 0.08) that was seen during this work.

Fig. 2: Growth of the Si^+ ion intensity on exposure to $2x10^{-8}$ torr of O_2 at 650 K. Ar^+ beam was 0.9 nA at 600 eV. AES spectra of the O(KLL) and Pt_{237} regions are also shown.

Fig. 3: Growth of the Si^+ ion intensity during O_2 TPD. 10 L of O_2 was adsorbed at 100 K and temperature programmed at 5.5 K/s to 1060 K. Ar^+ beam = 1.5 nA at 600 eV. The arrow marks the onset temperature (~500 K) of mobility of O(a) on Pt(111) [5].

Fig. 4: Decline of Si^+ and SiO^+ ion intensities on heating in vacuum above 1100 K. The sample was previously oxidized during a number of oxygen adsorption experiments with $^{18}O_2$. Ar^+ beam = 1.5 nA at 600 eV.

Fig. 5: SIMS spectra of an oxidized surface before and after H_2 treatment (1200 K, $2x10^{-8}$ torr). The amount of SiO_x was below AES detectability. Ar^+ beam = 1.8 nA at 600 eV.

Fig. 6: Changes in (a) SIMS impurity ion intensities, (b) "silicon oxide" O/Pt_{237} AES ratio and (c) oxygen desorption areas as function of

pretreatment. O = Oxidised at 700 K with 1×10^{-7} torr of O_2 for 900 sec. R = Reduced at 1200 K with 2×10^{-8} torr of H_2 for 200 secs. C = sputtered clean and annealed at 1200 K for 500 secs. After each pretreatment, 10 L of O_2 was adsorbed at 100 K and temperature programmed at 5.5 K/s until 1000 K to generate the TPD spectra. After each oxidation pretreatment the sample was flashed to 1000 K to remove any adsorbed oxygen, before performing the AES and SIMS scans.

Fig. 7: Changes in SIMS impurity ion intensities and O_2 desorption areas as function of consecutive oxygen adsorption/desorption cycles. In each case 10 L of O_2 was adsorbed at 100 K and temperature programmed at 5.5 K/s, to 1000 K. Before run #7 the sample was reduced in 2×10^{-8} torr of H_2 at 1200 K for 200 sec. Each of the O_2 desorption areas (and the total) in the first run are arbitrarily normalized to 100. Ar^+ beam = 0.8 nA at 600 eV.

Fig. 8: Changes in SIMS impurity ion intensities and O_2 desorption area as a function of consecutive O_2 adsorption/desorption cycle. 10 L of O_2 was adsorbed at 100 K and the sample was heated at a rate of 5.5 K/s to 1000 K. No SiO_x impurity was detectable in AES after run #7 ($O/Pt_{237} < 0.01$). Each of the O_2 desorption areas (and the total) in the first run are arbitrarily normalized to 100. Ar^+ ion = 1.5 nA at 600 eV.

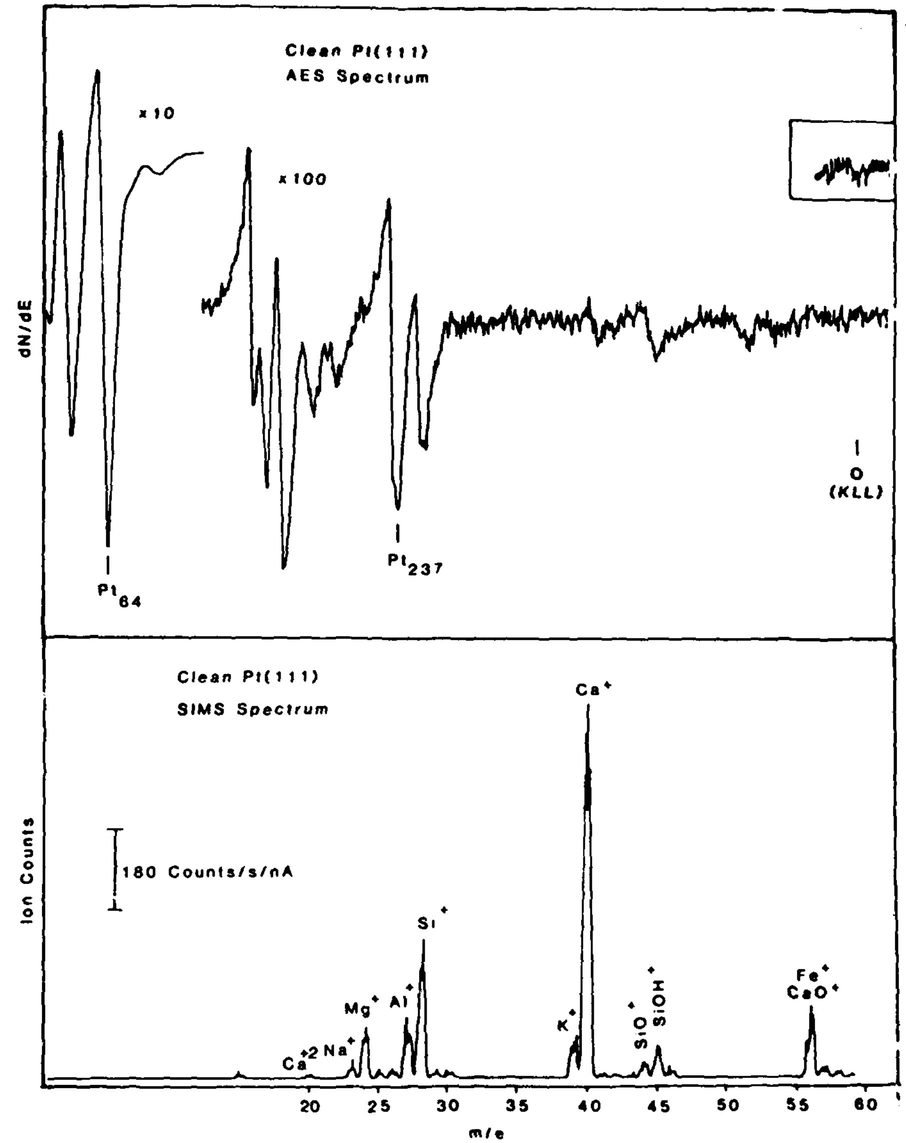

Fig. 1

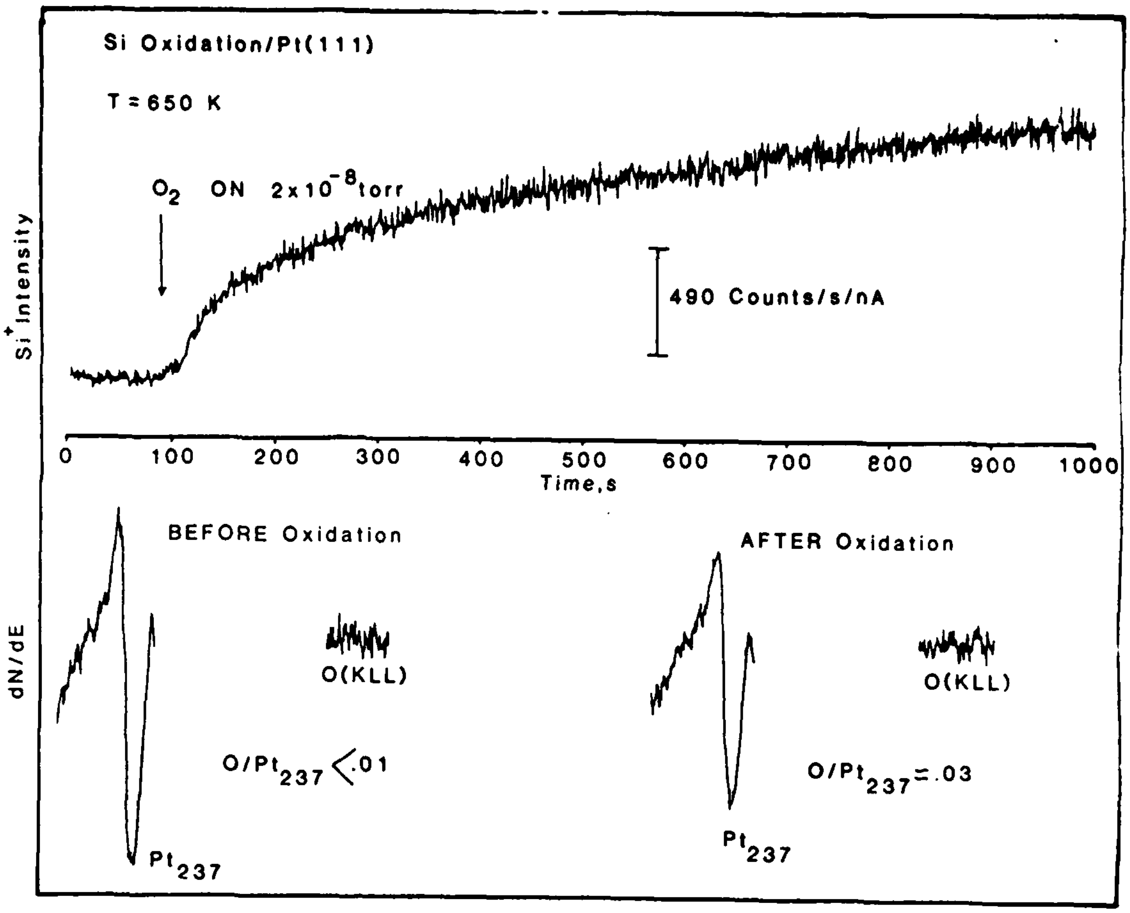

Si Oxidation/Pt(111)
T = 650 K
O_2 ON 2×10^{-8}torr
490 Counts/s/nA
Si^+ Intensity
0
100
200
300
400
500
600
700
800
900
1000
Time,s
BEFORE Oxidation
AFTER Oxidation
dN/dE
O(KLL)
O(KLL)
$O/Pt_{237} < .01$
$O/Pt_{237} = .03$
Pt_{237}
Pt_{237}

Fig 2

3

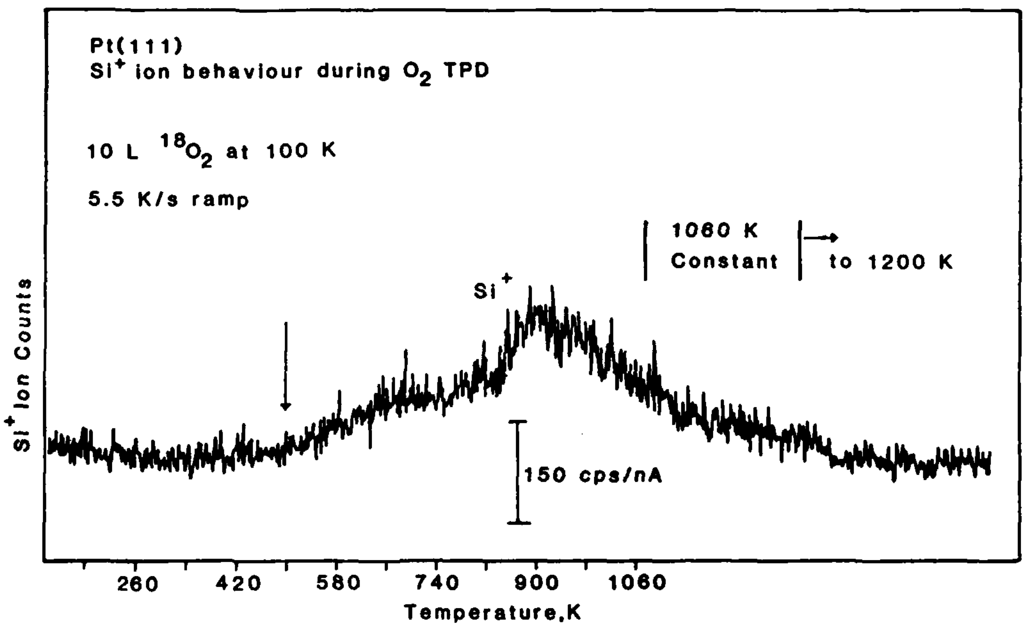

Pt(111)
Si^+ ion behaviour during O_2 TPD
10 L $^{18}O_2$ at 100 K
5.5 K/s ramp
1060 K
Constant
to 1200 K
Si^+
Si^+ Ion Counts
150 cps/nA
260
420
580
740
900
1060
Temperature,K

Fig. 3

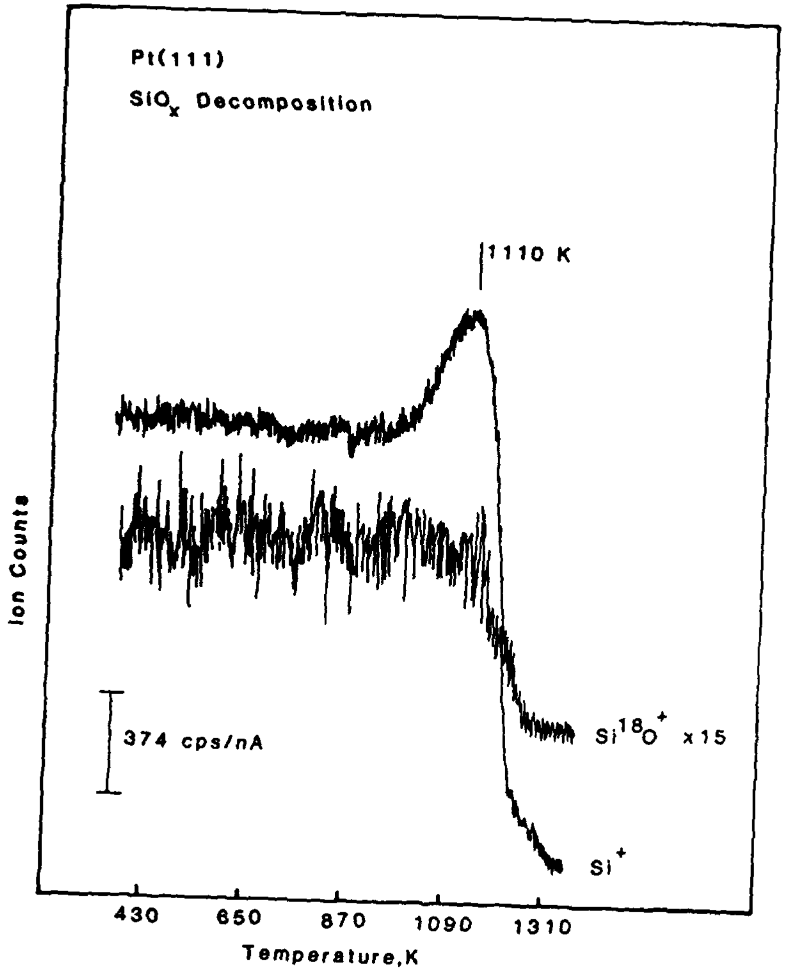

Pt(111)
SiOx Decomposition
1110 K
374 cps/nA
Si18O+ x15
Si+
Ion Counts
430
650
870
1090
1310
Temperature,K

Fig 4

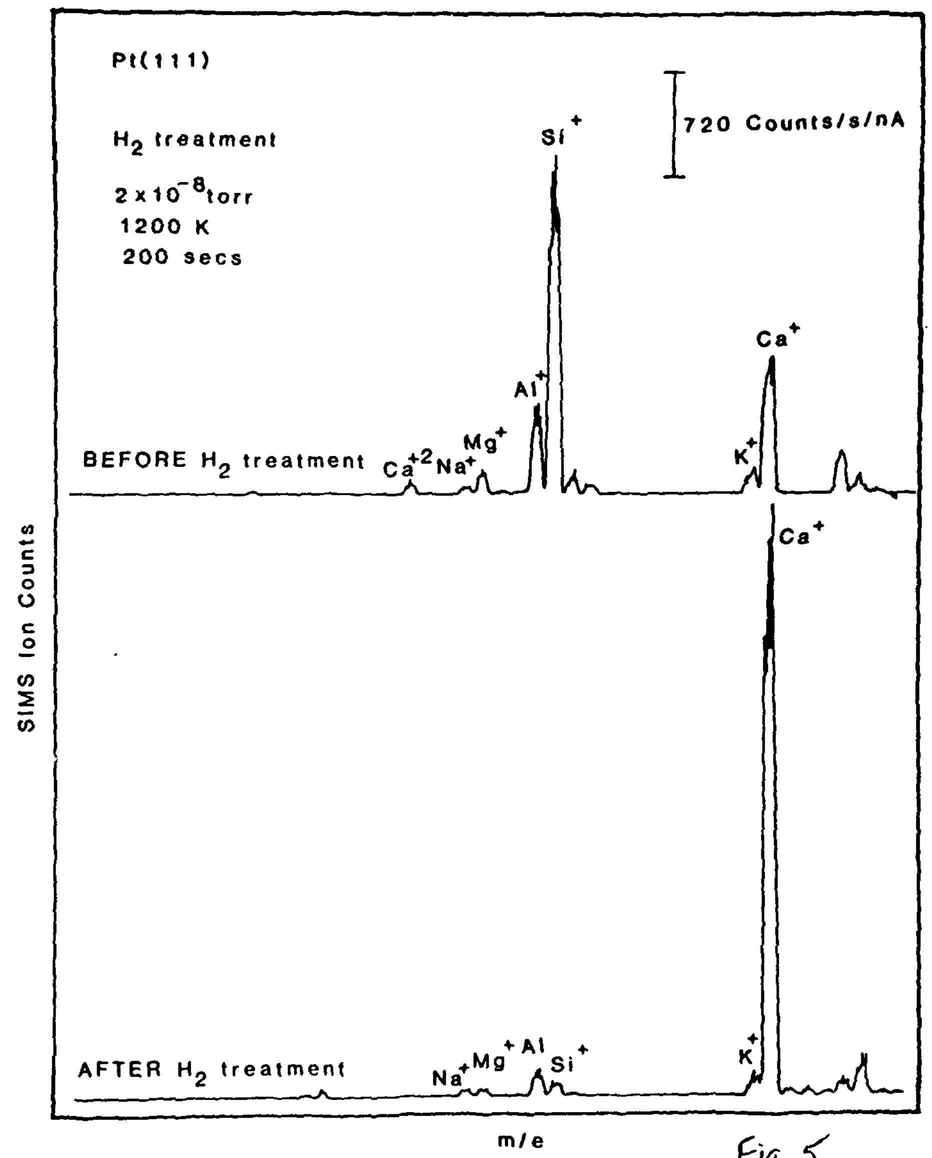

Pt(111)
H2 treatment
2x10-8torr
1200 K
200 secs
720 Counts/s/nA
Si+
Al+
Ca+
K+
Ca+2
Na+
Mg+
BEFORE H2 treatment
AFTER H2 treatment
SIMS Ion Counts
m/e

Fig. 5

7

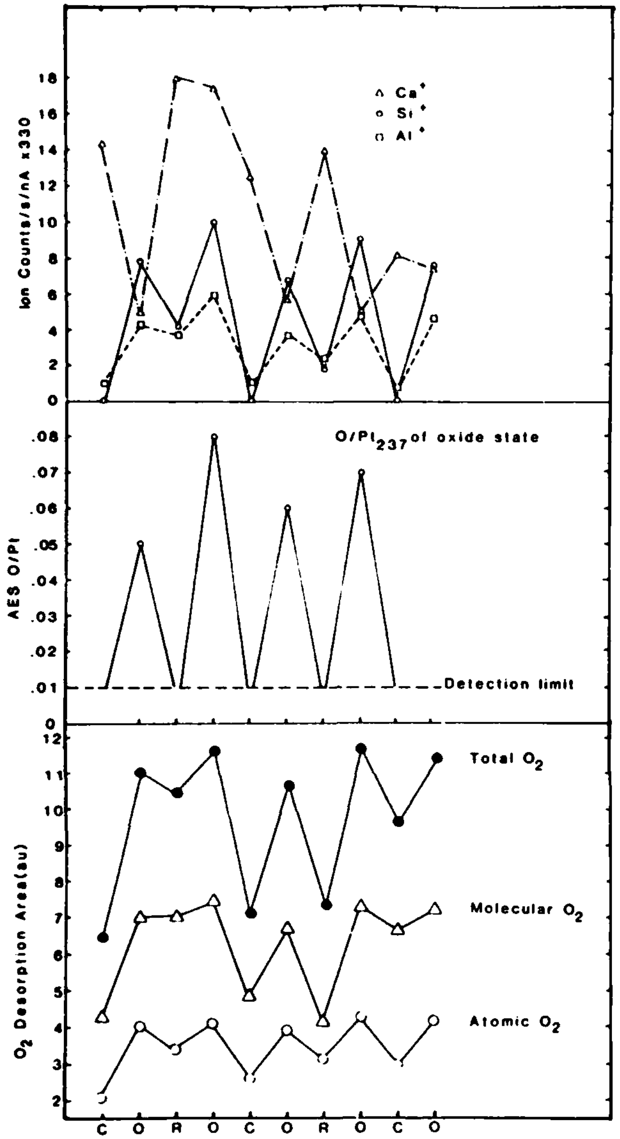

Ion Counts/s/nA x330
Ca+
Si+
Al+
AES O/Pt
O/Pt237 of oxide state
Detection limit
O2 Desorption Area(au)
Total O2
Molecular O2
Atomic O2
C O R O C O R O C O

Fig. 6

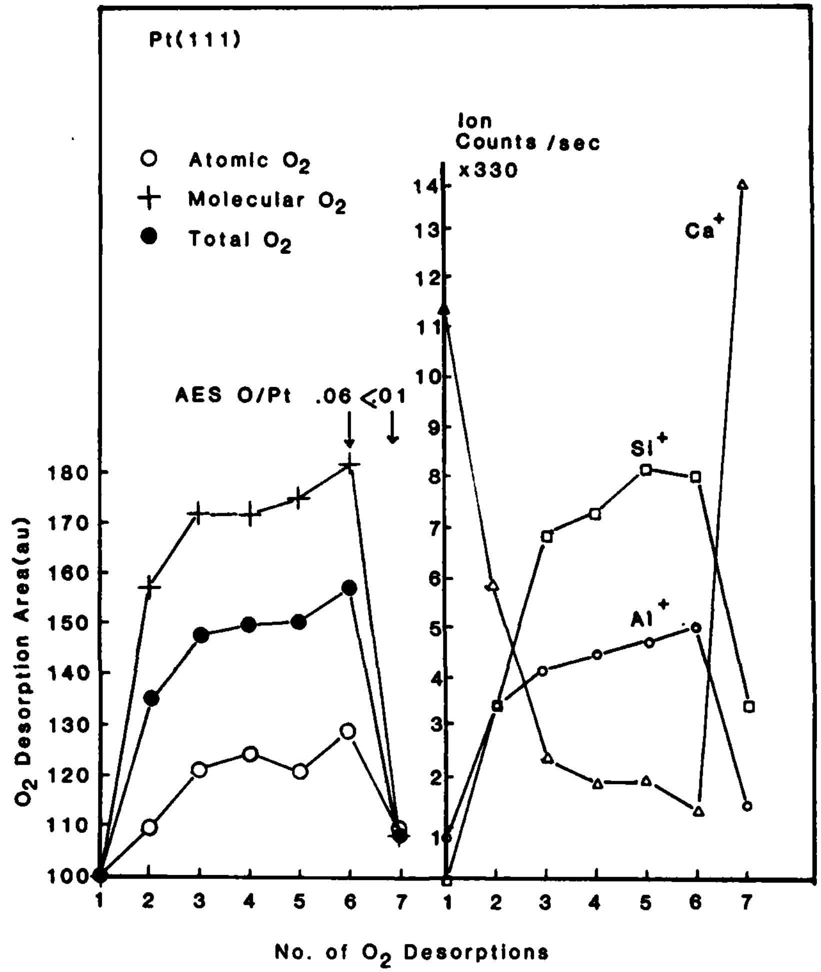

Pt(111)
Atomic O2
Molecular O2
Total O2
AES O/Pt .06 <01
O2 Desorption Area(au)
Ion Counts /sec x330
Ca+
Si+
Al+
No. of O2 Desorptions

Fig. 7

(3)

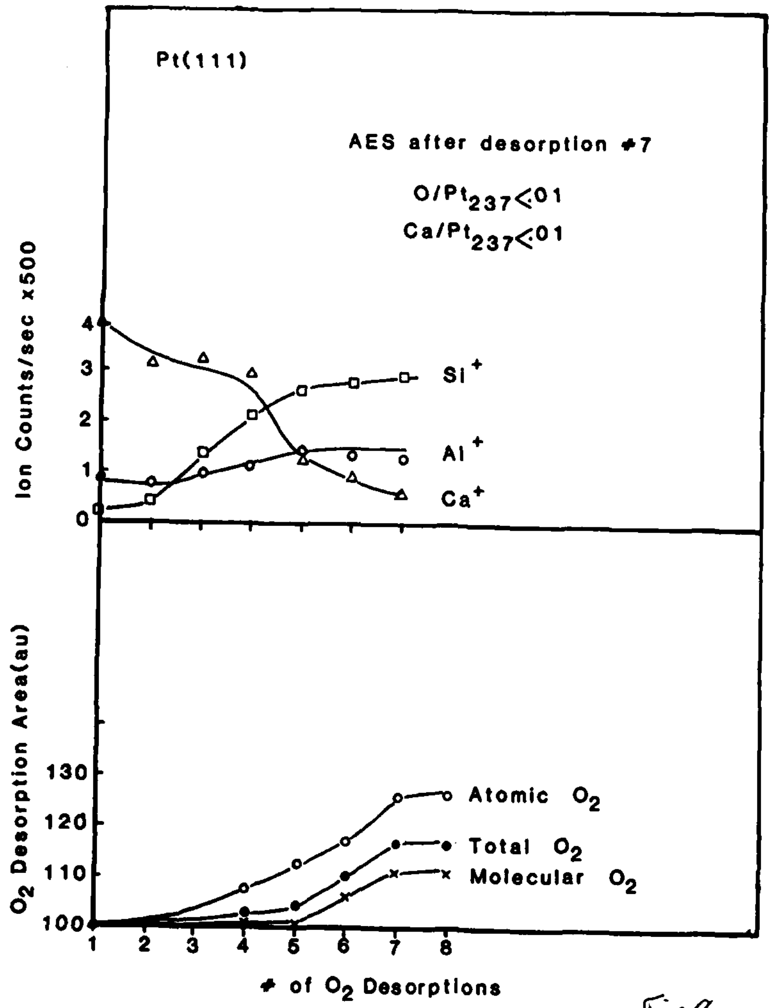
Pt(111)
AES after desorption #7
O/Pt237<01
Ca/Pt237<01
Si+
Al+
Ca+
Ion Counts/sec x500
0
1
2
3
4
O2 Desorption Area(au)
100
110
120
130
Atomic O2
Total O2
Molecular O2
1
2
3
4
5
6
7
8
# of O2 Desorptions

Fig 8

ABSTRACTS DISTRIBUTION LIST, 056/625/629

Dr. F. Carter
Code 6132
Naval Research Laboratory
Washington, D.C. 20375

Dr. Richard Colton
Code 6112
Naval Research Laboratory
Washington, D.C. 20375

Dr. Dan Pierce
National Bureau of Standards
Optical Physics Division
Washington, D.C. 20234

Dr. R. Stanley Williams
Department of Chemistry
University of California
Los Angeles, California 90024

Dr. R. P. Messmer
Materials Characterization Lab.
General Electric Company
Schenectady, New York 22217

Dr. Robert Gomer
Department of Chemistry
James Franck Institute
5640 Ellis Avenue
Chicago, Illinois 60637

Dr. Ronald Lee
R301
Naval Surface Weapons Center
White Oak
Silver Spring, Maryland 20910

Dr. Paul Schoen
Code 5570
Naval Research Laboratory
Washington, D.C. 20375

Dr. John T. Yates
Department of Chemistry
University of Pittsburgh
Pittsburgh, Pennsylvania 15260

Dr. Richard Greene
Code 5230
Naval Research Laboratory
Washington, D.C. 20375

Dr. L. Kesmodel
Department of Physics
Indiana University
Bloomington, Indiana 47403

Dr. K. C. Janda
California Institute of Technology
Division of Chemistry and Chemical
Engineering
Pasadena, California 91125

Dr. E. A. Irene
Department of Chemistry
University of North Carolina
Chapel Hill, Northc Carolina 27514

Dr. Adam Heller
Bell Laboratories
Murray Hill, New Jersey 07974

Dr. Martin Fleischmann
Department of Chemistry
Southampton University
Southampton 509 5NH
Hampshire, England

Dr. John W. Wilkins
Cornell University
Laboratory of Atomic and
Solid State Physics
Ithaca, New York 14853

Dr. Richard Smardzewski
Code 6130
Naval Research Laboratory
Washington, D.C. 20375

Dr. H. Tachikawa
Chemistry Department
Jackson State University
Jackson, Mississippi 39217

ABSTRACTS DISTRIBUTION LIST, 056/625/629

Dr. G. A. Somorjai
Department of Chemistry
University of California
Berkeley, California 94720

Dr. J. Murday
Naval Research Laboratory
Surface Chemistry Division (6170)
455 Overlook Avenue, S.W.
Washington, D.C. 20375

Dr. J. B. Hudson
Materials Division
Rensselaer Polytechnic Institute
Troy, New York 12181

Dr. Theodore E. Madey
Surface Chemistry Section
Department of Commerce
National Bureau of Standards
Washington, D.C. 20234

Dr. J. E. Demuth
IBM Corporation
Thomas J. Watson Research Center
P.O. Box 218
Yorktown Heights, New York 10598

Dr. M. G. Lagally
Department of Metallurgical
and Mining Engineering
University of Wisconsin
Madison, Wisconsin 53706

Dr. R. P. Van Duyne
Chemistry Department
Northwestern University
Evanston, Illinois 60637

Dr. J. M. White
Department of Chemistry
University of Texas
Austin, Texas 78712

Dr. D. E. Harrison
Department of Physics
Naval Postgraduate School
Monterey, California 93940

Dr. W. Kohn
Department of Physics
University of California, San Diego
La Jolla, California 92037

Dr. R. L. Park
Director, Center of Materials
Research
University of Maryland
College Park, Maryland 20742

Dr. W. T. Peria
Electrical Engineering Department
University of Minnesota
Minneapolis, Minnesota 55455

Dr. Keith H. Johnson
Department of Metallurgy and
Materials Science
Massachusetts Institute of Technology
Cambridge, Massachusetts 02139

Dr. S. Sibener
Department of Chemistry
James Franck Institute
5640 Ellis Avenue
Chicago, Illinois 60637

Dr. Arnold Green
Quantum Surface Dynamics Branch
Code 3817
Naval Weapons Center
China Lake, California 93555

Dr. A. Wold
Department of Chemistry
Brown University
Providence, Rhode Island 02912

Dr. S. L. Bernasek
Department of Chemistry
Princeton University
Princeton, New Jersey 08544

Dr. P. Lund
Department of Chemistry
Howard University
Washington, D.C. 20059

ABSTRACTS DISTRIBUTION LIST, 056/625/629

Dr. J. E. Jensen
Hughes Research Laboratory
3011 Malibu Canyon Road
Malibu, California 90265

Dr. J. H. Weaver
Department of Chemical Engineering
and Materials Science
University of Minnesota
Minneapolis, Minnesota 55455

Dr. W. Goddard
Division of Chemistry
California Institute of Technology
Pasadena, California 91125

Dr. A. Reisman
Microelectronics Center of North Carolina
Research Triangle Park, North Carolina
27709

Dr. M. Grunze
Laboratory for Surface Science and
Technology
University of Maine
Orono, Maine 04469

Dr. J. Butler
Naval Research Laboratory
Code 6115
Washington D.C. 20375

Dr. L. Interante
Chemistry Department
Rensselaer Polytechnic Institute
Troy, New York 12181

Dr. Irvin Heard
Chemistry and Physics Department
Lincoln University
Lincoln University, Pennsylvania 19352

Dr. K.J. Klaubunde
Department of Chemistry
Kansas State University
Manhattan, Kansas 66506

Dr. W. Knauer
Hughes Research Laboratory
3011 Malibu Canyon Road
Malibu, California 90265

Dr. C. B. Harris
Department of Chemistry
University of California
Berkeley, California 94720

Dr. F. Kutzler
Department of Chemistry
Box 5055
Tennessee Technological University
Cookesville, Tennessee 38501

Dr. D. DiLella
Chemistry Department
George Washington University
Washington D.C. 20052

Dr. R. Reeves
Chemistry Department
Renssaeler Polytechnic Institute
Troy, New York 12181

ABSTRACTS DISTRIBUTION LIST, 056/625/629

Dr. R. G. Wallis
Department of Physics
University of California
Irvine, California 92664

Dr. D. Ramaker
Chemistry Department
George Washington University
Washington, D.C. 20052

Dr. J. C. Hemminger
Chemistry Department
University of California
Irvine, California 92717

Dr. T. F. George
Chemistry Department
University of Rochester
Rochester, New York 14627

Dr. G. Rubloff
IBM
Thomas J. Watson Research Center
P.O. Box 218
Yorktown Heights, New York 10598

Dr. Horia Metiu
Chemistry Department
University of California
Santa Barbara, California 93106

Dr. W. Goddard
Division of Chemistry
California Institute of Technology
Pasadena, California 91125

Dr. J. T. Keiser
Department of Chemistry
University of Richmond
Richmond, Virginia 23173

Dr. R. W. Plummer
Department of Physics
University of Pennsylvania
Philadelphia, Pennsylvania 19104

Dr. E. Yeager
Department of Chemistry
Case Western Reserve University
Cleveland, Ohio 41106

Dr. N. Winograd
Department of Chemistry
Pennsylvania State University
University Park, Pennsylvania 16802

Dr. Roald Hoffmann
Department of Chemistry
Cornell University
Ithaca, New York 14853

Dr. A. Steckl
Department of Electrical and
Systems Engineering
Rensselaer Polytechnic Institute
Troy, NewYork 12181

Dr. G. H. Morrison
Department of Chemistry
Cornell University
Ithaca, New York 14853

Dr. P. Hansma
Physics Department
University of California
Santa Barbara, California 93106

Dr. J. Baldeschwieler
California Institute of Technology
Division of Chemistry
Pasadena, California 91125

TECHNICAL REPORT DISTRIBUTION LIST, GEN

	No. Copies
Office of Naval Research Attn: Code 413 800 N. Quincy Street Arlington, Virginia 22217	2
Dr. Bernard Douda Naval Weapons Support Center Code 5042 Crane, Indiana 47522	1
Commander, Naval Air Systems Command Attn: Code 310C (H. Rosenwasser) Washington, D.C. 20360	1
Naval Civil Engineering Laboratory Attn: Dr. R. W. Drisko Port Hueneme, California 93401	1
Defense Technical Information Center Building 5, Cameron Station Alexandria, Virginia 22314	12
DTNSRDC Attn: Dr. G. Bosmajian Applied Chemistry Division Annapolis, Maryland 21401	1
Dr. William Tolles Superintendent Chemistry Division, Code 6100 Naval Research Laboratory Washington, D.C. 20375	1
Dr. David Young Code 334 NORDA NSTL, Mississippi 39529	1
Naval Weapons Center Attn: Dr. Ron Atkins Chemistry Division China Lake, California 93555	1
Scientific Advisor Commandant of the Marine Corps Code RD-1 Washington, D.C. 20380	1
U.S. Army Research Office Attn: CRD-AA-IP P.O. Box 12211 Research Triangle Park, NC 27709	1
Mr. John Boyle Materials Branch Naval Ship Engineering Center Philadelphia, Pennsylvania 19112	1
Naval Ocean Systems Center Attn: Dr. S. Yamamoto Marine Sciences Division San Diego, California 91232	1

END

FILMED

12-85

DTIC